

Sb and Bi on GaAs(110): Substrate-stabilized overlayer structures studied with scanning tunneling microscopy

J. C. Patrin, Y. Z. Li, M. Chander, and J. H. Weaver

Department of Materials Science and Chemical Engineering, University of Minnesota, Minneapolis, Minnesota 55455

(Received 28 February 1992)

The growth structures for Sb and Bi films on GaAs(110) have been studied for thicknesses of 0.5–50 monolayers (ML) with annealing to temperatures as high as 600 K. Antimony films exhibit layered structures with $\sim 6\text{-}\text{\AA}$ heights but also disordered surface features for coverages up to ~ 10 ML when grown at 300 K. Annealing to 500 K produces orientationally ordered films that contain grains with striped domain walls and two differently oriented superstructures. These superstructures can be explained in terms of a Moiré effect in which the $\langle 001 \rangle$ direction of the pseudocubic Sb(110) plane is rotated by $+7^\circ$ or -7° from the substrate $[1\bar{1}0]$ direction. Sb undergoes a semiconductor-semimetal transition when the film thickness reaches $\sim 15\text{ \AA}$. By 20-ML deposition, the ability of the substrate to dictate surface structure is lost. Films grown at 300 K are polycrystalline with randomly oriented basal planes. Annealing to 600 K creates large crystallites with basal planes parallel to the substrate surface. For Bi overlayers on GaAs(110), the first layer is epitaxial but two-dimensional islands form on the 1×1 layer at 300 K. These islands are $\sim 7\text{ \AA}$ in height and exhibit two differently oriented superstructures. As for Sb, this superstructure reflects a Moiré effect. For Bi/GaAs, the $\langle 001 \rangle$ direction of the Bi pseudocubic (110) plane is rotated by $+10^\circ$ or -10° from the substrate $[1\bar{1}0]$ direction. The islands coalesce to form large, highly anisotropic crystallites having a periodic superstructure at 4-ML coverage. Bi crystallites are formed after 50-ML deposition at 300 K with elongation along the substrate $[1\bar{1}0]$ direction.

I. INTRODUCTION

The growth modes of metals and nonmetals on semiconductors have received considerable attention recently because there is increasing interest in control over the various growth parameters and because the scanning tunneling microscope (STM) allows direct imaging of the overlayer structures.¹ Particular emphasis has been on the structures of the semimetals Sb and Bi on GaAs(110) because they form ordered interfaces free of intermixing.^{2–8} Feenstra and Mårtensson have shown that the first Sb layer is epitaxial on GaAs(110) but also that there are vacancies in that layer and small clusters are formed on it.² For coverages > 1 ML, a layered structure formed on the epitaxial layer but its surface appeared to be disordered.³ Each layer is $\sim 6\text{ \AA}$ thick, corresponding to the stacking of three atomic planes. STM results for 1 ML of Bi on GaAs(110) (Ref. 4) have shown that the first layer grows epitaxially with misfit dislocations every $\sim 25\text{ \AA}$ in the $[1\bar{1}0]$ direction.⁴ The presence of misfit dislocations has been associated with the larger atomic size of Bi compared to Sb and the need to relieve strain.

In this paper, we focus on Sb and Bi growth on GaAs(110), with emphasis on the changing structures as a function of the amount of material deposited and the annealing temperatures used. The coverages investigated spanned the range from the first ordered monolayer to the substrate mediated structures to the intrinsic structure exposing (111) surfaces. The temperature ranged from 300 K to the desorption temperatures of Sb and Bi. For Sb/GaAs(110), the low coverage results are in agreement with those of Feenstra and co-workers,^{2,3} showing a

1×1 epitaxial layer. Subsequent growth at 300 K of ~ 4 ML produces islands that are $\sim 6\text{ \AA}$ high with nucleation on terraces prior to completion of lower levels. Surface flattening is enhanced by annealing, and orientationally ordered grains are produced. Superstructures within the grains reflect Moiré patterns due to island alignment with respect to the substrate.⁹ Nonintersecting domain walls form in these grains due to lattice compression. The grains are continuous over monatomic steps. The domain walls are also continuous through substrate monatomic steps and Sb terrace steps. The Sb layers exhibit a semiconductor-semimetallic transition when they are $\sim 15\text{ \AA}$ thick. Growth to 20–40 ML produces polycrystalline Sb films at 300 K with basal planes that are generally not parallel to the substrate surface, but annealing to $\sim 600\text{ K}$ yields large Sb crystallites with basal planes parallel to the substrate. Hence, growth on GaAs(110) involves two differently oriented rhombohedral structures because of the influence of the substrate-overlayer interface.

For Bi/GaAs(110), the deposition of the equivalent of 2 ML at 300 K results in an epitaxial layer and then the formation of $\sim 7\text{-}\text{\AA}$ high islands on the epitaxial layer. These two-dimensional (2D) islands also have superstructures with 21- \AA periodicity oriented $+55^\circ$ or -55° relative to the substrate $[1\bar{1}0]$ direction. Additional Bi deposition results in island coalescence so that large crystallites are formed. These anisotropic crystallites exhibit a superstructure that can be modeled as a Moiré effect in which the $\langle 001 \rangle$ direction of the Bi pseudocubic (110) plane is rotated by $+10^\circ$ or -10° from the substrate $[1\bar{1}0]$ direction. For a 50-ML Bi deposition, crystallites

are formed that are preferentially elongated in the substrate $[1\bar{1}0]$ direction.

II. EXPERIMENT

The STM experiments were conducted in an ultrahigh-vacuum chamber containing reverse view optics for low-energy electron diffraction (LEED) and a Park Scientific Instruments scanning tunneling microscope. GaAs(110) surfaces were prepared by cleaving $2 \times 3 \times 10 \text{ mm}^3$ sample posts that were Zn doped at $1 \times 10^{19} \text{ cm}^{-3}$. Electrochemically etched tungsten tips were cleaned *in situ* by electron bombardment. Sb and Bi were evaporated from resistively heated Ta boats, and the amount of metal deposited was determined with a quartz-crystal microbalance. The pressure remained below 1×10^{-10} Torr during evaporation (operating pressure of 6×10^{-11} Torr). One monolayer of Sb (Bi) corresponds to 2.7 \AA (3.1 \AA) assuming $8.85 \times 10^{14} \text{ atoms cm}^{-2}$. Although we will adopt the monolayer representation for characterizing the amount of material condensed, layer-by-layer growth is not implied. Indeed, as the STM images will show, the growth is more complex.

In most cases, the samples were held at 300 K during deposition, but some results were obtained for samples held at 575 K during deposition. Annealing involved heating for ~ 1 h, including a 15-min warmup period. Typically, imaging could commence within 1 h after the heater was turned off. Temperatures were measured with a chromel-alumel thermocouple attached to the sample holder. They were verified with an optical pyrometer. Calibration of the piezoelectric scanner was done using the GaAs(110) lattice and monatomic steps on the surface.

All images were taken in the constant-current mode with currents of 0.1–1.0 nA and bias voltages of $\pm(0.2\text{--}3)$ V. The images are displayed with the $[1\bar{1}0]$ direction being 135° from the $+x$ direction, except where noted. The crystal planes and directions for Sb and Bi are given in the pseudocubic notation. We have also included the rhombohedral indexing where needed for clarity. For a detailed discussion of the structure of Sb and Bi and the relationship of these indexing conventions, we refer the reader to the thorough paper by Jona.¹⁰ As he showed, the rhombohedral structure can be approximated by a pseudocubic structure. Additional motivation for using the pseudocubic notation comes from the fact that cubic structures for As, Sb, and Bi can be produced by high pressure and the influence of the substrate may tend to stabilize this cubic phase. Although intriguing, the present results cannot distinguish between the two structures, but none of the conclusions are influenced by the slight ambiguity.

III. RESULTS AND DISCUSSION

A. 0.4–8-ML Sb/GaAs(110): Substrate-mediated structures

Figure 1(a) shows an atomic resolution STM image obtained after 0.5 ML of Sb had been deposited on GaAs(110) at 575 K. This curvature-enhanced image

shows rows of Sb atoms parallel to the $[1\bar{1}0]$ substrate direction. The spacing between rows is $\sim 5.6 \text{ \AA}$ along the $[001]$ direction, as demonstrated previously.² Imaging with this sample voltage, -2.32 V , reveals Sb atoms bonded to surface Ga atoms.² The effect of Sb deposition is to unrelax the surface layer of GaAs to its bulklike termination. Thus, the two inequivalent Sb adatoms in the unit cell are nearly equidistant from the surface plane, even though they are not identical electronically. Sb clusters can form on top of the 1×1 terraces at 300 K,² but they are not present for growth at 575 K. Likewise, fewer clusters form at terrace edges compared to 300-K growth.² While there are vacancies in the terraces, the vacancy number can be reduced by depositing more than the equivalent of 1 ML of Sb at 300 K and annealing to $\sim 600 \text{ K}$. This process also removes excess Sb. Even for growth at 575 K, the edges of the 1×1 regions are irregular in shape.

Figure 1(b) shows a STM image obtained after the equivalent of 1.5-ML Sb deposition. In this case, growth involved deposition followed by annealing to 600 K to produce a single well-ordered 1×1 monolayer¹¹ and then the deposition of another 0.5 ML of Sb at 300 K. The Sb island that represents most of the image is $\sim 6 \text{ \AA}$ or three layers higher than the underexposed 1×1 Sb layer at the right. Such triple-layer islands cover only about 20% of the surface. Small bright clusters are also evident on the island surface. The small dark areas reflect irregularities in the surface layer of the island, probably associated with incomplete growth of the topmost layer (discussed below). These island surfaces contain fewer clusters than those produced for higher coverages, and the edges of the islands are more distinct. This probably reflects the fact that the defect-free epitaxial monolayer acts as a good substrate for the growth of the first multilayer.

Figure 1(c) is a large-scale STM image obtained after the deposition of ~ 4 ML of Sb ($\sim 3.6 \times 10^{15} \text{ atoms/cm}^2$), following the same growth procedure used for the 1.5-ML deposition [Fig. 1(b)]. Up to four different height multilayers can be seen on this image, each $\sim 6 \text{ \AA}$ thick. Such growth is referred to as modified Stranski-Krastonov or monolayer plus simultaneous multilayer (MSM) growth since layers nucleate before preceding layers are completed.¹² Models of MSM growth assume that the lateral diffusion of Sb is insufficient to produce complete layers. Such multilayers are thermodynamically less stable than planar layers, but they are kinetically favored. Disordered clusters are also present on the surface. The upper right corner shows the 1×1 epilayer with only small amounts of second-layer Sb. Detailed analysis of the surface of the thicker multilayers shows increasing cluster density and roughness than for Fig. 1(b), presumably because the multilayer islands act as less perfect templates than the annealed 1×1 epilayer.

Figure 1(d) shows a crystalline film with terraces produced by annealing the Sb overlayer of Fig. 1(c) to 375 K. After annealing, the clusters disappeared, the island surfaces were much smoother, and the overall topography was more regular. The upper right corner shows a triple-layer island on a lower triple-layer terrace. Within each multilayer, darker regions can be readily observed.

It is likely that they are formed from the disordered depressions of Fig. 1(b). Seen in cross section, the lighter areas of the island are $\sim 6 \text{ \AA}$ above the lower terrace and the darker areas are $\sim 4 \text{ \AA}$ higher. The edges of the interconnected ordered arrays are irregular with no preferential orientation.

The $2300 \times 2300 \text{ \AA}^2$ image of Fig. 1(e) shows that annealing 4 ML of Sb to 500 K produces larger, better-ordered multilayers. Again, the height difference be-

tween the lighter and darker areas in the lower half of the image is 2 \AA or one layer of Sb. In addition, the central portion of the figure shows a second multilayer island that is 6 \AA higher than the region surrounding it. This island also has 2-\AA depressions. The growth of complete multilayers near higher level multilayer islands indicates that Sb diffuses from the higher islands. Such flattening can be understood from free-energy arguments.

Figure 1(f) schematically depicts a multilayer region on

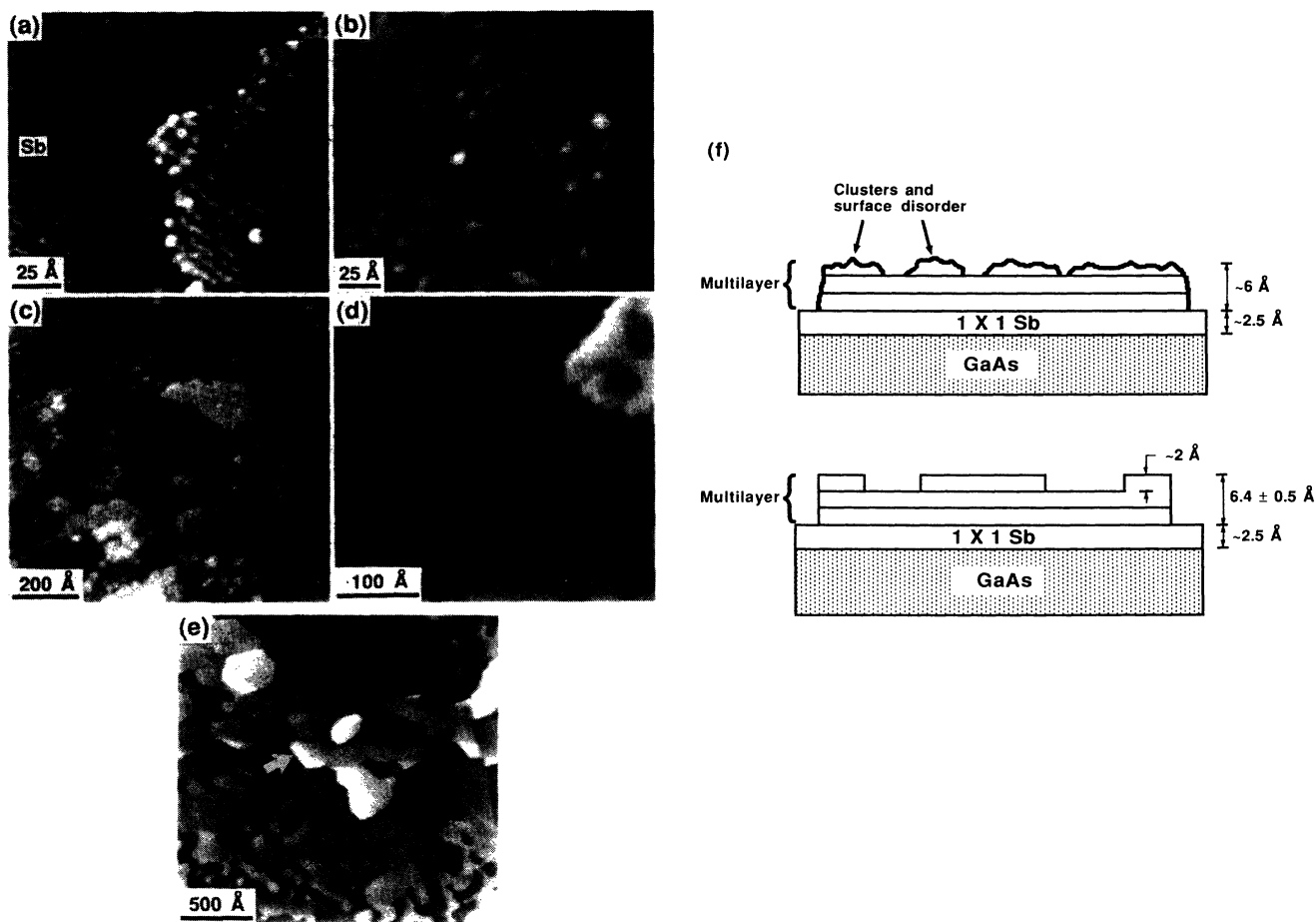


FIG. 1. (a) A curvature-enhanced atomic resolution image obtained after the equivalent of 0.5 ML of Sb was deposited at 575 K on GaAs(110). The islands at the left and right exhibit the 1×1 epitaxial Sb structure. Growth at 300 K produces clusters on the 1×1 structure and at the edges of the 1×1 islands, but the cluster number density is significantly reduced for growth at 575 K. (b) $200 \times 200\text{-\AA}^2$ image showing the growth of an Sb multilayer on the 1×1 Sb epilayer (the latter is the underexposed region at the right of the image). The multilayer surface shows disorder due to depressions (darker regions) and Sb clusters (bright spots). This layer is $\sim 6 \text{ \AA}$ thick, corresponding to three layers of Sb. (c) STM image after the equivalent of 4 ML Sb was deposited on GaAs(110) at 300 K. The upper right corner shows the 1×1 epilayer with bright spots that correspond to islands of the first multilayer. The numbers draw attention to four successive multilayers. Each is $\sim 6 \text{ \AA}$ thick, corresponding to a triple layer of Sb. Small clusters are also apparent on each multilayer surface. (d) A $400 \times 400\text{-\AA}^2$ image obtained after annealing the surface of Fig. 1(c) to 375 K. Annealing eliminates the small Sb clusters and enhances surface ordering. The darker regions are recessed by a single Sb layer from the surrounding regions. The brighter area at upper right shows a second trilayer where the darker portions are one layer thinner. (e) STM image after annealing 4 ML of Sb at 500 K. The dark areas in the lower half reflect ordered regions one Sb layer thinner than the brighter areas surrounding them. The upper portion shows a large island that is 6.4 \AA thick and derived from a triple layer of Sb, as indicated by the arrow. Within it, the darker areas are two layers thick. Comparison to (d) shows that annealing enhances layer ordering by forming a complete atomic layer near the trilayer island. (f) A schematic cross section depicting Sb multilayer growth on a 1×1 epilayer on GaAs(110). The upper panel reveals the disorder apparent in the images of (b) and (c). Annealing produces the better ordered structure of the lower panel with double and triple layers of Sb on the 1×1 layer.

a 1×1 layer that is in contact with the substrate. Growth at 300 K produces these multilayers but it also produces the small clusters and depressions shown as irregularities at the top of Fig. 1(f). It is important to note that the disordered Sb clusters coalesce and transform to ordered three-layer-thick multilayers at some critical stage in the growth sequence, even for growth at 300 K. Continued deposition produces additional islands, as in Fig. 1(c), each with $\sim 6 \text{ \AA}$ height and derived from three layers of Sb. Annealing enhances surface ordering, as depicted at the bottom of Fig. 1(f), and clear separation into two- and three-layer structures with a reduction in the number of steps to minimize step energy costs.

Figure 2(a) shows a $2500 \times 2400 \text{ \AA}^2$ image obtained after the sample of Fig. 1(c) was annealed to 525 K for 2 h. Similar results were obtained for lower annealing temperatures and longer times. At this stage, the surface topography was much more regular with no exposed 1×1 areas and few second- or third-layer islands. The first-layer islands formed a network with homogeneous $6.4 \pm 0.5 \text{ \AA}$ thickness over large regions of the surface. Within this overlayer there were grains with easily distinguished boundaries. The superstructures, visible as parallel lines in gray scale, were oriented $+40^\circ$ or -40° from the $[1\bar{1}0]$ substrate direction, as labeled. The spacing between the lines is $25 \pm 2 \text{ \AA}$ and the peak-to-peak corrugation was $\sim 0.4 \text{ \AA}$ for a sample bias of 1.0 V. The superstructure can be modeled as a Moiré effect in which the $\langle 001 \rangle$ direction of the Sb pseudocubic (110) plane [or, equivalently, the rhombohedral $(10\bar{1})$ plane] is rotated by $+7^\circ$ or -7° with respect to the substrate $[1\bar{1}0]$ direction.⁹

Domain walls (DW's) are also formed, visible as bright lines that generally begin at one end of a grain and terminate at the other. They are roughly parallel to one another and do not intersect. Such striped domain walls reflect strain associated with the compression of an adsorbed layer.¹³ Our STM images for Sb/GaAs(110) show that the domain walls form in regions of complete uniformly thick multilayers. Such domain walls and superstructures were also produced by lower annealing temperatures [they were present in a $\sim 500\text{-\AA}$ band below the second multilayer in Fig. 1(e)]. A domain wall was also found bisecting an isolated island $\sim 500 \text{ \AA}$ in size having clearly evident superstructures. The domain-wall corrugation was voltage dependent, ranging from $\sim 2 \text{ \AA}$ at a sample voltage of 0.2 V to $\sim 0.2 \text{ \AA}$ at a sample voltage of 2.5 V. This indicates that the domain-wall appearance is largely an electronic effect that is associated with an underlying structural difference.

Lines of defects (D) define the grain boundaries of Fig. 2(a). The defect diameter is $\sim 20 \text{ \AA}$ but the size is also somewhat bias dependent. Defects occasionally appear within a grain as well, where they can serve to terminate a single domain wall. The arrow at the right center of Fig. 2(a) draws attention to a region devoid of periodic superstructures or domain walls. It was not surrounded by defects, and it may still have structural disorder. The dark region in the upper right corresponds to a $\sim 2\text{-\AA}$ -deep depression where the third layer of the 6.4-\AA multilayer had not formed.

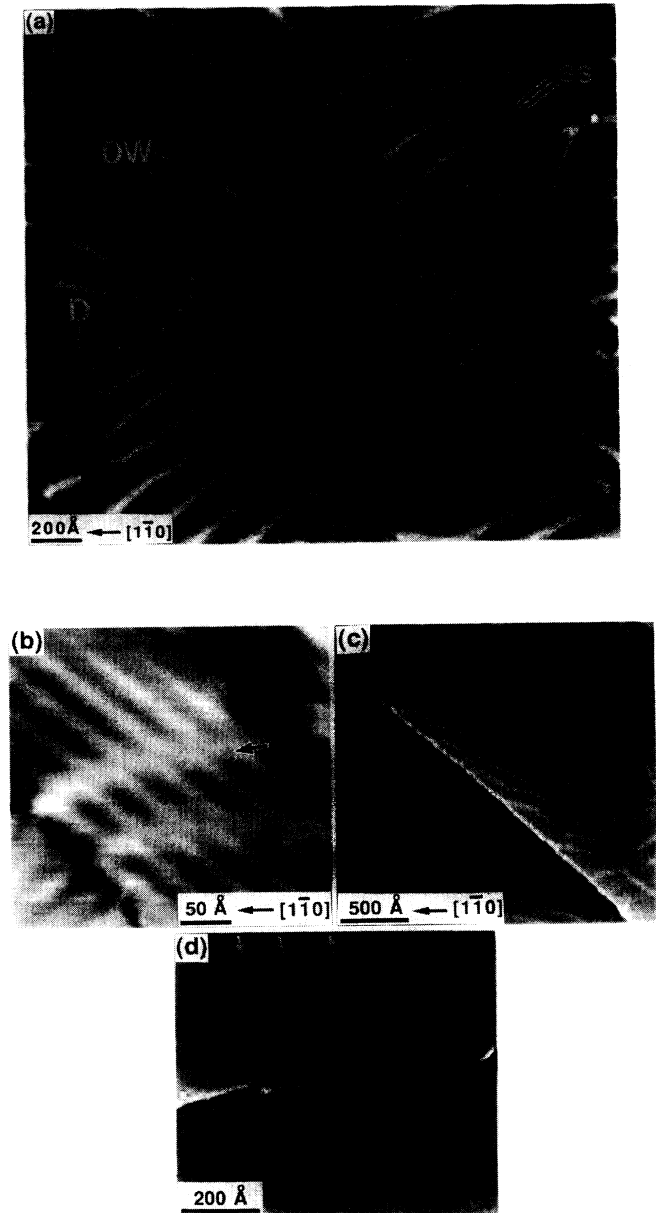


FIG. 2. (a) STM image obtained after annealing 4 ML of Sb to 525 K for 2 h. Differently oriented superstructures (SS) aligned $+40^\circ$ or -40° relative to the substrate $[1\bar{1}0]$ direction are apparent in the grains as straight lines in gray scale. As discussed, the superstructure reflects a Moiré effect. Defects (D) of $\sim 20\text{-\AA}$ size define the grain boundaries. Periodically spaced striped domain walls (DW) are formed within each grain due to strain in the Sb overlayer. The dark region at upper right is a monolayer depression. The arrow draws attention to a region with no apparent order. (b) STM image of a portion of (a) showing a grain defined by defects with domain walls and a superstructure that is oriented 40° relative to $[1\bar{1}0]$. There is a phase shift of 180° as the superstructure passes through the domain wall. (c) A curvature-enhanced STM image showing that the grain boundaries and the domain walls are continuous over a monatomic substrate step which runs diagonally through the image. (d) A curvature-enhanced STM image showing that the domain walls (marked by arrows) continue through a 6.4-\AA -high multilayer step in the Sb overlayer.

Figure 2(b) represents a high-resolution image where the two superstructure orientations, the domain walls, and the grain boundaries are evident. This particular image was chosen because it shows that the superstructure has a phase shift of 180° as it passes through the domain wall. As will be illustrated below, the phase shift can be modeled by producing dislocations in any of the pseudocubic $\langle 110 \rangle$ directions. Figure 2(c) shows that the Sb grains are continuous over monatomic substrate steps.

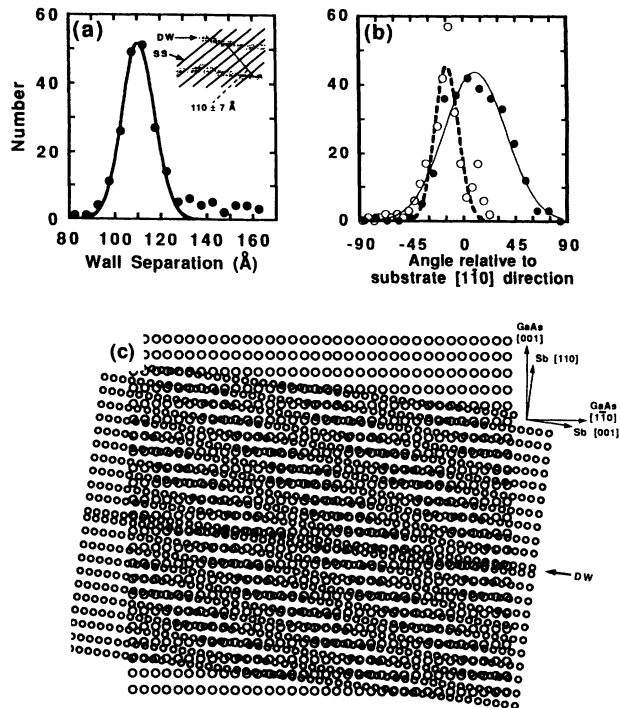


FIG. 3. (a) A distribution of domain walls as a function of their separation derived from images such as Fig. 2(a). The mean separation was 110 ± 7 Å. The inset shows how the domain wall (DW) separation was defined with respect to the superstructure (SS). (b) The angular distribution of domain walls for the two differently oriented grains. The domain-wall angle is given with respect to the substrate $[1\bar{1}0]$ direction. The solid (dashed) line is a Gaussian fit to the distribution of domain walls for grains containing superstructures oriented $+40^\circ$ (-40°) relative to $[1\bar{1}0]$. The peak for the grains containing the superstructure oriented $+40^\circ$ (-40°) is $+10^\circ$ (-15°). (c) Moiré pattern generated between the Sb pseudocubic (110) lattice and the GaAs(110) surface. For simplicity, each Ga-As pair was represented by a single circle. The Sb lattice was rotated 7° clockwise from the GaAs array, producing a superstructure with a separation of ~ 24 Å, as observed experimentally. The phase shift observed for the superstructures as they passed through the domain wall (DW) was modeled by creating a dislocation of $a/2\langle 110 \rangle$ in the Sb lattice. (The GaAs substrate directions are given along with the Sb pseudocubic directions in the upper right corner.) From (a), these dislocations are spaced every 110 ± 7 Å.

The $2\text{-}\text{Å}$ -high step of Fig. 2(c) runs $\sim 135^\circ$ from the $+x$ axis. The lines of defects that define the perimeter of the grains and the domain walls are continuous across the step. The image of Fig. 2(d) also illustrates the continuous character of the domain walls as they pass through a $6.4\text{-}\text{Å}$ multilayer step and even through the oval grain boundary at lower right. These observations indicate that the domain walls and the grain boundaries (consisting of defects) probably extend to the 1×1 Sb layer and are not inhibited by surface defects and steps.

Insight into the character of the domain walls can be obtained by measuring their separation and their lengths for overlayers annealed to 525 K. The separation was determined by measuring the distance perpendicular to the superstructure, as depicted in the inset of Fig. 3(a). The measurements were taken 200 Å from the grain boundaries at $200\text{-}\text{Å}$ intervals to avoid possible interactions between the domain walls and grain boundaries. A Gaussian fit indicates the mean separation is 110 Å (standard deviation ± 7 Å). The onset of domain-wall formation in large uniformly thick multilayers and the periodic separation between the domain walls indicate that they serve to relieve strain in the overlayer.

To determine whether the domain walls had preferred orientations, we measured their directions for the differently oriented grains. The domain-wall orientation is important because the compression of the overlayer occurs perpendicular to the domain-wall direction. Figure 3(b) shows the distribution of domain-wall orientations for the two differently oriented grains, together with Gaussian fits to the experimental results. For grains with superstructures oriented $+40^\circ$ (-40°), the domain-wall orientation has a maximum at approximately $+10^\circ$ (approximately -15°) from the substrate $[1\bar{1}0]$ direction. This suggests that the direction of the domain walls occurs primarily along the $\langle 001 \rangle$ direction of the (110) pseudocubic Sb plane. Therefore, the compression for Sb occurs mainly in the pseudocubic $\langle 110 \rangle$ direction. Using this, we can model a domain wall by creating a dislocation of $a/2\langle 110 \rangle$ in the pseudocubic Sb (110) surface. Figure 3(c) shows a Moiré pattern generated from the substrate (simplified in the figure by using a single symbol per unit cell to reflect a Ga and As pair) and the pseudocubic (110) Sb surface. The latter was rotated by -7° from the substrate $[1\bar{1}0]$ direction. The Sb lattice also includes a domain wall (dislocation) near the middle of the figure. The periodic superstructure is reproduced as well as a phase shift of 180° for the superstructure as it passes through the domain wall. This phase shift corresponds to that observed experimentally in Fig. 2(b). Although this simple model reproduces the phase shift across the domain wall, the atomic positions across the domain wall and its width within one unit cell should not be inferred.

Annealing Sb multilayers to 550 K exposed large regions of the epitaxial 1×1 layer on GaAs(110). Some terraces were observed that were up to ~ 18 Å or three triple layers high, containing grains with domain walls and superstructures. The existence of the domain walls and the superstructures and the persistence of the triple-layer structures indicate that the substrate was able to influence the surface layer even when it was 18 Å away.

STM images acquired after the equivalent of ~ 8 ML of Sb had been deposited and annealed to 450 K revealed atomically flat islands on regions exhibiting domain walls and periodic superstructures. These islands were ~ 4 Å thick, in contrast to those observed for thinner films where the multilayer height was ~ 6 Å. Some layers had triangular or hexagonal symmetry, suggesting a change in the growth pattern of the rhombohedral overlayer. In addition, the domain walls and superstructures from the lower-coverage multilayer structures did not persist. These observations are particularly interesting because they signal the transition from a substrate-stabilized overlayer exposing surfaces with rectangular symmetry to one exposing the low-energy (111) surfaces of the rhombohedral structure. The transition from the substrate-stabilized structure to one exposing (111) surfaces with hexagonal symmetry was clearly seen by low-energy electron diffraction (LEED).⁵ In particular, fractional order spots adjacent to integer order spots were observed for a 3-ML Sb coverage and annealing to 475 K. The LEED pattern showed the gradual appearance of two different rotated hexagonal domains on a ring structure as the overlayer thickened.

B. 10–40-ML Sb/GaAs(110): Transition to intrinsic growth structures

Images obtained after the equivalent of 10 ML of Sb deposition on GaAs(110) at 300 K show a surface having small clusters, as at lower coverages, but the 6-Å layered structures were not apparent. The absence of distinct multilayers probably reflects the fact that each successive multilayer acts as an increasingly imperfect template, together with the change in growth pattern to one in which the surface layer is close packed. Annealing to 475 K produced large layered crystallites that were parallel to the substrate, as shown in Fig. 4. Their hexagonal symmetry indicates that they exposed (111) planes. Each layer is 3.9 ± 0.4 Å higher than the layer below, corresponding to the stacking of two planes in the [111] rhombohedral direction. The existence of double-layer steps is not surprising because Sb (as well as Bi) form puckered double layers.¹⁰ The double layers arise because each atom forms pyramidal bonds with its three nearest neighbors and the next-nearest neighbors are in the adjacent layer.¹⁰ These crystallites had no preferred azimuthal orientation. The left portion of Fig. 4 shows a stack of four such double layers (~ 16 Å high) with well-defined linear edges. The right portion shows a hexagonal region that is two double layers lower than the surrounding terrace. These structures are clearly different from those observed at low coverage in terms of their stacking (double layers rather than triple layers) and their symmetry. Again, this indicates that the substrate-mediated structures are stabilized up to a critical thickness after which it is energetically favorable for the Sb structures to expose (111) planes, even at the expense of a grain boundary

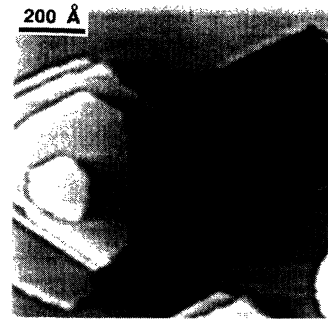


FIG. 4. STM image obtained after 10-ML Sb deposition on GaAs(110) followed by annealing to 475 K. The left portion shows an island consisting of four Sb bilayers. Each bilayer is ~ 4 Å high. The Sb rhombohedral $\langle 111 \rangle$ direction is normal to the surface. The hexagonal pit at the right is two bilayers or ~ 8 Å deep.

or transition layer for the two differently oriented rhombohedral structures. (As noted above, we cannot exclude the possibility that the low coverage structure is cubic rather than pseudocubic, but the existence of a change in growth is clear nonetheless.)

Figure 5(a) shows a STM image for 20 ML of Sb deposited at 300 K. In this case, the overlayer is highly irregular with many layers easily discerned. Also evident are irregular clusters near the edges of the platelets. Moreover, the basal planes of the crystallites are randomly oriented azimuthally as well as out of the GaAs surface. Comparison to the equivalent results for 10-ML deposition indicates crystallites are much more easily formed for the thicker films. This is consistent with a previous reflection high-energy electron-diffraction (RHEED) study¹⁴ where the substrate pattern gradually disappeared with coverage until 20 ± 3 ML, at which point a diffraction pattern appeared. Annealing the 20-ML film to 500 K produced larger grains, as shown in Fig. 5(b). Many of the crystallites produced by annealing had basal planes that were parallel to the substrate surface, as in Fig. 4. There were also regions in which the $\langle 111 \rangle$ direction was not normal to the surface, and, in this case, there was extensive faceting. The lower portion of Fig. 5(b) shows such regions where there are ~ 20 steps in a staircase. These steps are nearly straight and parallel and the terraces are very narrow. Annealing to ~ 600 K enhanced grain growth, producing a surface where all of the crystallites were parallel to the surface, as in Fig. 5(c). The crystallite edges were generally straight and intersected at 60° to produce triangular corners. Associated with these steps were screw dislocations with the Burgers vector normal to the surface. The height between successive layers was 3.9 ± 0.4 Å, corresponding to two layers perpendicular to the $\langle 111 \rangle$ rhombohedral direction. Heating above ~ 625 K led to Sb desorption. In this case, the images showed crystallites surrounded by large regions of the 1×1 epilayer on GaAs(110).

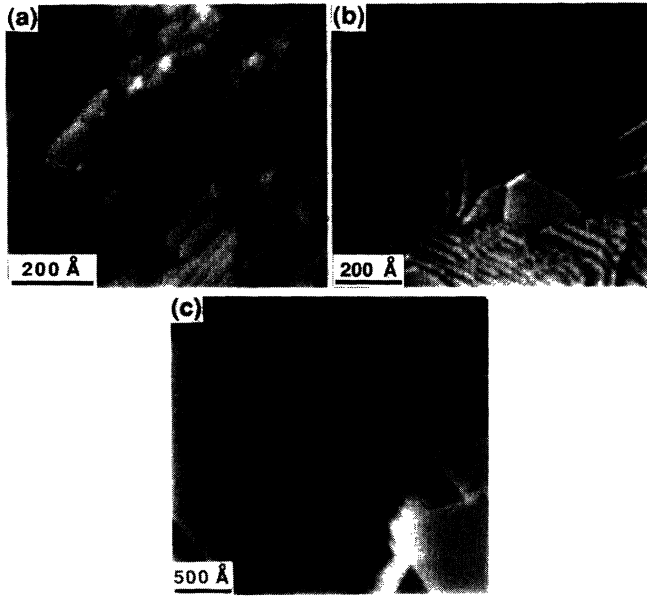


FIG. 5. (A) $800 \times 800\text{-}\text{\AA}^2$ STM image of 20 ML of Sb deposited at 300 K. The triangular structures expose $\{111\}$ surfaces that are randomly oriented. (b) $1000 \times 1000\text{-}\text{\AA}^2$ curvature-enhanced image obtained after annealing (a) to 500 K. The top portion shows Sb crystallites with basal planes parallel to the substrate. Each layer is $\sim 4\text{ \AA}$ thick, and ten layers can be seen in this image. The bottom portion shows a stack of layers in which the $\langle 111 \rangle$ direction is not normal to the surface. (c) STM image showing 20 ML of Sb after annealing to 600 K. The $\langle 111 \rangle$ direction of the overlayer is normal to the surface. In general, the surface is very flat, but triangular-shaped structures can be observed that are related to pairs of clockwise and counterclockwise screw dislocations. In addition, triangular-shaped pits can also be observed (not shown here). Each layer is $3.9 \pm 0.4\text{ \AA}$ thick, corresponding to two Sb layers.

C. Sb/GaAs(110): Semiconductor-semimetal transition

Sandomirskii¹⁵ predicted that semiconductor-semimetal transitions would be observed for thin films where the transition would be induced by a quantum size effect that reflects the thickness of the film. In the semiconducting state, the energy gap E_g was predicted to depend quadratically on the film thickness, namely $E_g = \Delta[(\bar{t})^2/t^2 - 1]$, where Δ is the overlap between the conduction and valence bands and \bar{t} is the thickness at which the gap vanishes. This relationship assumes that the thin film is infinite in the lateral direction. Bismuth has been the semimetal generally used to study this effect¹⁶ because of the small overlap between the conduction and valence bands and the small effective masses of the electrons and holes. However, it has been difficult to produce atomically smooth surfaces and films with precisely known thicknesses. Annealed Sb films on GaAs(110) have the advantage of growing in a distinct layered structure that is atomically flat.

Figure 6(a) shows a STM image for Sb/GaAs(110)

where region A is a 1×1 Sb layer and regions B and C are ~ 6.4 and $\sim 12.8\text{ \AA}$ higher [see the sketch of Fig. 1(f)]. Figure 6(b) shows representative I - V measurements taken on each layer. From the I - V measurements, the 1×1 Sb layer has a band gap of $1.2 \pm 0.1\text{ eV}$, in agreement with previous studies.^{2,3} The $6.4\text{-}\text{\AA}$ layer has a band gap of $0.6 \pm 0.2\text{ eV}$, and the $12.8\text{-}\text{\AA}$ layer has a band gap of $0.15 \pm 0.1\text{ eV}$. The band gap is the region of zero conductivity in the I - V spectra. Each band gap is an average of up to 30 measurements long with the statistical error. Linear extrapolation using the latter two values would predict that the Sb film would become semimetallic when it is $\sim 15\text{ \AA}$ thick. This is in reasonable agreement with calculations using bulk parameters, i.e., 0.2 eV for the overlap of the valence band and the conduction band and the effective masses of electrons and holes.¹⁷

D. Bi/GaAs(110): Substrate-mediated and intrinsic structures

Figure 7(a) shows a $450 \times 450\text{ \AA}^2$ image obtained after 2 ML of Bi had been deposited at 300 K (sample bias 1.47 V). These growth conditions produce an epitaxial 1×1 layer on which 2D islands form. As for Sb/GaAs(110),

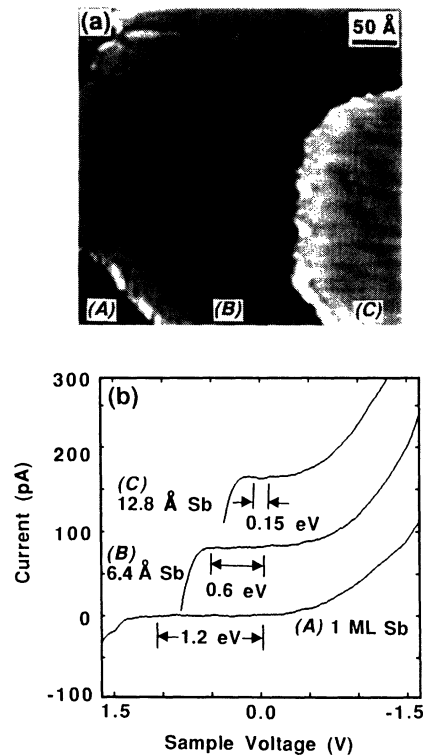


FIG. 6. (a) $400 \times 400\text{-}\text{\AA}^2$ STM image for ~ 3 ML of Sb annealed to 425 K. The image shows two successive ~ 6 -high- \AA -trilayers (B and C) on the 1×1 layer (A). (b) Representative I - V curves labeled A , B , and C correspond to measurements taken at the 1×1 Sb layer (A), the $6.4\text{-}\text{\AA}$ trilayer (B), and the $12.8\text{-}\text{\AA}$ trilayer (C) showing a reduction in the band gap as the Sb layer thickens. Sb undergoes a semiconductor-semimetal transition at $\sim 15\text{ \AA}$.

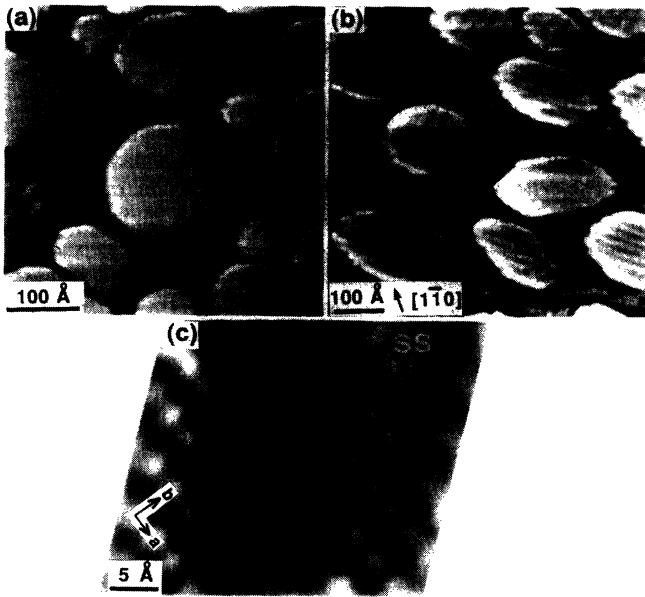


FIG. 7. (a) $450 \times 450\text{-}\text{\AA}^2$ curvature-enhanced image showing 2-ML Bi deposition at 300 K (sample bias of 1.47 V). The lower level reflects the 1×1 epitaxial layer with periodic misfit dislocations (arrows) spaced about 25 \AA in the $[1\bar{1}0]$ direction. The islands on the epilayer are $\sim 7\text{ \AA}$ high and nearly isotropic. (b) $750 \times 750\text{-}\text{\AA}^2$ image obtained with a sample bias of -0.1 V that reveals the two differently oriented periodic superstructures on the island surface. The superstructure is oriented $+55\%$ or -55% from the substrate $[1\bar{1}0]$ direction. This image has not been drift-corrected. (c) Drift-corrected atomic resolution image of $\sim 7\text{-}\text{\AA}$ -high Bi island. The lattice spacing is 3.4 and 4.5 \AA in the a and b directions. Notice that the rows shift by one half the lattice spacing as they pass through the superstructure (SS).

the 1×1 layer induces the nearly complete unrelaxation of the substrate surface.¹⁸ The dark lines in the epitaxial layer are associated with misfit dislocations that run approximately parallel to the $[001]$ direction, as identified by the arrows in Fig. 7(a). McLean *et al.*⁴ showed that these misfit dislocations are spaced about 25 \AA apart in the $[1\bar{1}0]$ direction and they attributed them to strain relief. The islands on the epilayer generally do not exceed $\sim 300\text{ \AA}$ in diameter and they are $7.0 \pm 0.5\text{ \AA}$ in height.¹⁹ The island surfaces are uniform, indicating that the misfit dislocations do not propagate through them.

Figure 7(b) shows a STM image of the same 2-ML Bi/GaAs(110) film obtained with a sample bias of -0.1 V (not corrected for drift). In this case, the epilayer is poorly resolved because it has a gap of 0.6 eV .⁴ Under these conditions, however, the periodic superstructures SS on the Bi islands are readily apparent. These superstructures are spaced every $\sim 21\text{ \AA}$ and they are oriented $+55^\circ$ or -55° from the substrate $[1\bar{1}0]$ direction. (The crystal orientation for this image is different than for the others.) The superstructure orientation is close to the angle between the $[1\bar{1}2]$ and $[1\bar{1}0]$ directions of the surface unit cell ($\pm 54.7^\circ$). These oriented superstructures may

produce the additional diffraction spots along the diagonals of the integer order beams reported in recent LEED studies for Bi on GaAs(110).^{6,7,20,21}

Figure 7(c) shows a drift-corrected atomic resolution image for an individual Bi island to illustrate the atom positions through the superstructure (SS). The Bi surface lattice has rectangular symmetry that corresponds to a pseudocubic (110) plane with lattice constants of $a = 3.3\text{ \AA}$ and $b = 4.8\text{ \AA}$ so that $b = \sqrt{2}a$.²² The $\sim 7\text{-}\text{\AA}$ island height would then correspond to the stacking of three layers in the pseudocubic $\langle 110 \rangle$ direction (the rhombohedral $[10\bar{1}]$ direction), as for Sb multilayers. The superstructure can be modeled again as a Moiré effect, but in this case the $\langle 001 \rangle$ direction of the Bi pseudocubic (110) lattice is rotated $+10^\circ$ or -10° from the $[1\bar{1}0]$ substrate direction. The angle of rotation was determined by the difference between the Bi pseudocubic $\langle 110 \rangle$ direction and the substrate $[001]$ direction from the STM images. In addition, the atoms shift by one half the lattice spacing in the $\langle 110 \rangle$ direction, as illustrated by the lines parallel to the a direction as they cross through the center region of Fig. 7(c). This effect was also observed for Sb on GaAs(110).⁹ It can be associated with the Moiré effect, but it also exhibits a voltage dependence, as discussed below.

Figure 8(a) shows a large-scale STM image obtained after 6 ML of Bi had been deposited at 300 K. Surprisingly, the 2D islands on the 1×1 epilayer have largely disappeared (this figure shows only one) and they have been replaced by large elongated crystallites. This image was chosen because it shows that the elongated crystallites are oriented approximately $+10^\circ$ or -10° with respect to the $[1\bar{1}0]$ substrate direction. They grow in layers, and cross sections from the STM images reveal that each layer is $\sim 4\text{ \AA}$ in height, corresponding to two layers perpendicular to the (110) pseudocubic plane [rhombohedral $(10\bar{1})$]. The deposition of 4 ML of Bi produced similar results. Hence, the 2D islands coalesce spontaneously to form large crystallites, even at 300 K, for depositions between 2 and 4 ML, sweeping large areas of the 1×1 epilayer free of 2D islands. We speculate that the 2D islands are metastable and atoms are readily detached at 300 K. The elongated multilayer crystallites are much more energetically favored so that the 2D islands yield to the elongated crystallites. From the STM images, the 2D islands are nearly isotropic in shape, whereas the crystallites are very anisotropic. Although both structures expose pseudocubic (110) surfaces, the 2D islands are three layers high, while the elongated crystallite heights are in multiples of two layers. Evidently, the shape of the growth structure is extremely dependent on the thickness.

Figure 8(b) demonstrates that the surfaces of the elongated Bi crystallites contain the same $21\text{-}\text{\AA}$ periodic superstructure as the 2D islands. The image of Fig. 8(b) was chosen because it shows a line of defects defining a grain boundary that is parallel to one of the superstructure orientations. Within each grain, the superstructures are oriented $+55^\circ$ or -55° from the $[1\bar{1}0]$ substrate direction. The corrugation of the periodic superstructure was $0.2\text{--}0.3\text{ \AA}$ for a sample bias of 1.0 V .

Figure 8(c) is an atomic resolution image of a typical region containing the superstructure where the superstructure is oriented -55° from the $[1\bar{1}0]$ direction. The atoms are spaced 3.25 and 4.66 Å apart in the a and b directions, respectively, in close agreement to atomic distances for the pseudocubic (110) plane [rhombohedral $(10\bar{1})$ plane], namely 3.29 and 4.746 Å.²² Inspection of Fig. 8(c) reveals that the spacing is constant and the rows are continuous through the superstructures, in contrast to Fig. 7(c) where the rows appear to shift as they pass through the superstructure. This is somewhat misleading, however, because the phase shift is dependent on the imaging conditions. This is demonstrated in Fig. 8(d) where the bottom half of the image was acquired at 30 mV and the top half was acquired at 90 mV. Thus, an electronic effect plays a role in dictating the apparent atomic positions.

Figure 8(e) shows a Moiré pattern generated using the substrate lattice (again simplified with one atom per unit

cell) and the (110) pseudocubic plane of Bi in which the Bi $\langle 001 \rangle$ direction is rotated 10° clockwise from the $[1\bar{1}0]$ substrate direction. The Moiré pattern reproduces the superstructure orientation of -55° with respect to $[1\bar{1}0]$ and spacing of ~ 21 Å. Figure 8(e) also shows that the Bi rows appear to be aligned with the substrate when the Bi rows are directly over the substrate rows, as observed experimentally in Figs. 7(c) and 8(d).

Figure 9 is a representative large-scale image obtained after 50 ML of Bi was deposited on GaAs(110) at 300 K. This surface is dominated by large crystallites that are oriented parallel to the $[1\bar{1}0]$ direction. Cross sections reveal that the height difference between successive layers is ~ 4 Å, corresponding to the stacking of two layers in the rhombohedral $\langle 111 \rangle$ direction and surface termination with (111) planes. LEED studies in this coverage regime showed hexagonal symmetry with a lattice constant comparable to the bulk value.^{19,20} The fact that Bi forms crystallites for all coverages at 300 K, whereas Sb crystal-

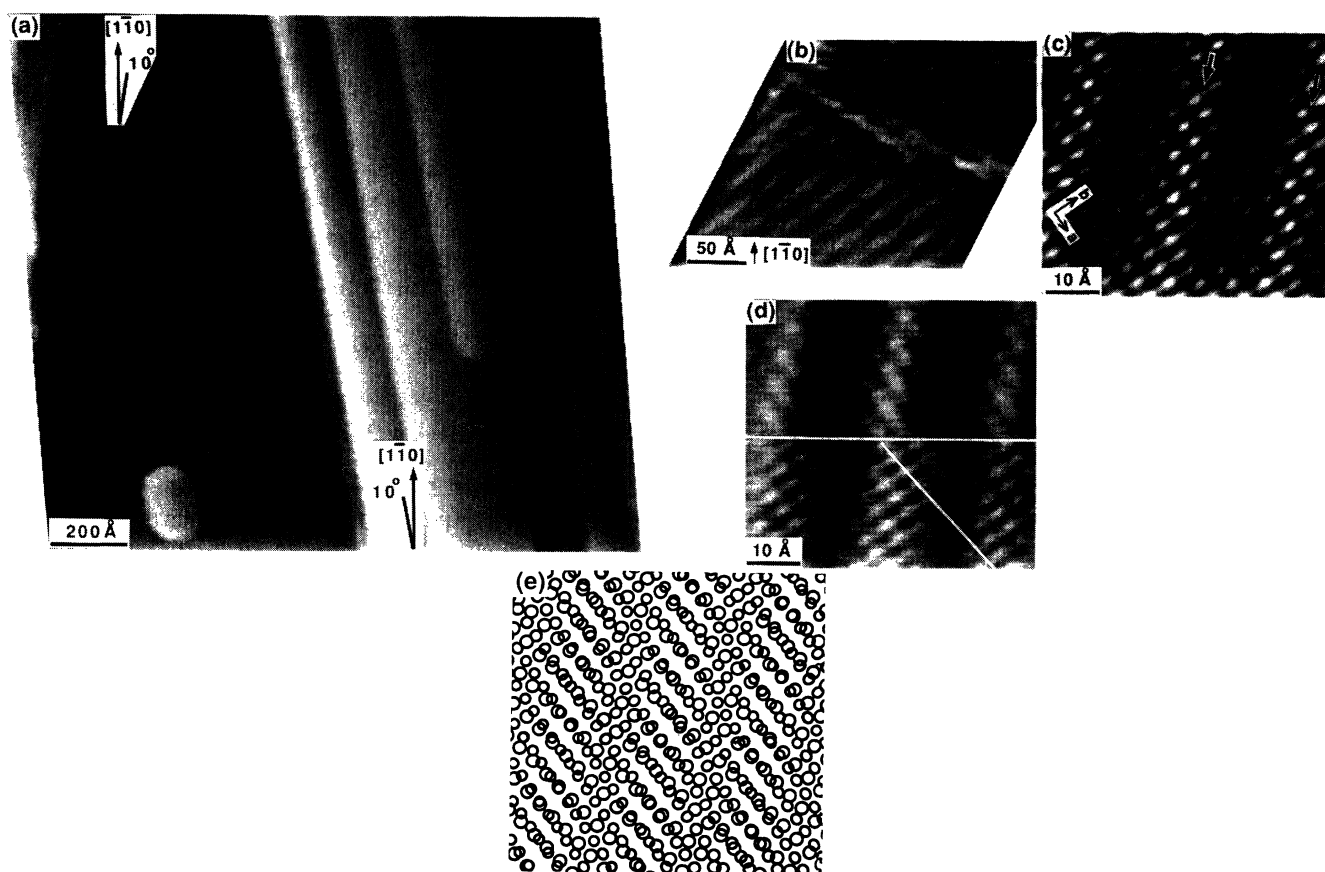


FIG. 8. (a) $1400 \times 1400\text{-}\text{\AA}^2$ image for 6-ML Bi deposition at 300 K. The image shows elongated Bi crystallites aligned $+10^\circ$ or -10° from the substrate $[1\bar{1}0]$ direction. Within the crystallites, there are 21-Å periodic superstructures oriented $+55^\circ$ or -55° from the $[1\bar{1}0]$ direction as in Fig. 7(b). Each step within the crystallite corresponds to a Bi bilayer (~ 4 Å). The isolated Bi island at the lower left corner of the figure is ~ 7 Å high. It also contains a periodic superstructure. (b) Higher-resolution image showing the two superstructure orientations separated by a line of defects. The superstructures are oriented either $+55^\circ$ or -55° from the $[1\bar{1}0]$ substrate direction. (c) Atomic resolution image of a Bi crystallite after 6 ML of Bi was deposited at 300 K. The atomic spacing is 3.25 Å along the a direction and 4.66 Å along the b direction. The arrows draw attention to the periodic superstructure. (d) Atomic resolution image showing the bias dependence for rows as they pass through the superstructure. The rows in the upper portion of the image appear to run straight through the superstructure (bias 90 mV), whereas those at the bottom appear to shift by one half the lattice spacing (bias 30 mV), as indicated by the white line. (e) Moiré pattern generated by rotating the $\langle 001 \rangle$ direction of the pseudocubic (110) Bi pseudocubic lattice by -10° relative to the $[1\bar{1}0]$ substrate direction. The superstructure appears as periodically spaced lines running -55° from the $[1\bar{1}0]$ substrate direction.

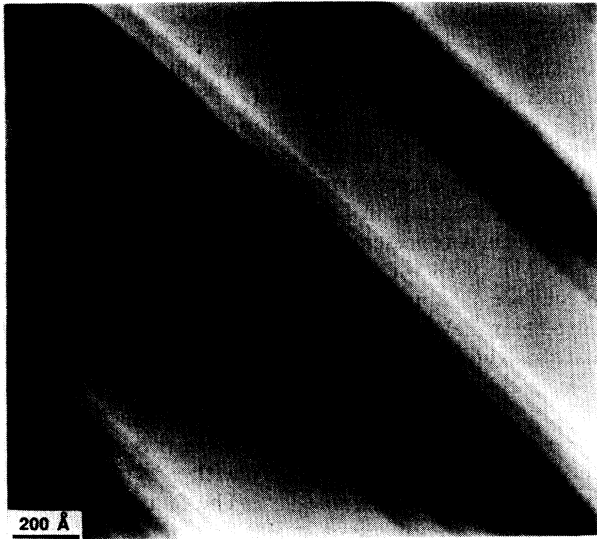


FIG. 9. STM image obtained after 50 ML of Bi deposition at 300 K. The Bi crystallites have atomically flat surfaces and elongate preferentially along the substrate $\langle 1\bar{1}0 \rangle$ direction. Each layer is ~ 4 Å thick, corresponding to stacking of two layers in the $\langle 111 \rangle$ rhombohedral direction.

lite formation required annealing, is probably due to the lower melting temperature of Bi (545 K versus 904 K for Sb).

In the above, we have described the structure of Bi as pseudocubic (rhombohedral). It should be noted that there are actually two Bi(110) pseudocubic planes with dimensions of 4.75 and 4.54 Å in the $\langle 110 \rangle$ directions and 6.57 Å in the $\langle 001 \rangle$ direction.^{10,23} The interlayer bond length of 3.47 Å and intralayer bond length of 3.1 Å make up the unit cell length in the $\langle 001 \rangle$ direction.²³ In our studies, we could not differentiate between the interlayer and intralayer distances and have assumed that we measured the average of the two. One possible reason that we could not observe a difference is that Bi (as well as Sb) forms a simple cubic phase at low coverage. Total-energy calculations reveal small energy differences between the rhombohedral and simple cubic structures. For example, there is only a 0.060-eV/atom difference between the energy minima in the rhombohedral and simple cubic structures of arsenic.²⁴ Such simple cubic structures for Sb and Bi have been observed at high pressure.^{23,25} While the existence of a simple cubic structure stabilized by the substrate cannot be ruled out, the conclusions of this paper are independent of such a slight change in the substrate-mediated overlayer.

IV. CONCLUSION

In this paper, we have examined the temperature- and coverage-dependent structures of Sb and Bi grown on GaAs(110). For low coverage, Bi overlayers and annealed Sb overlayers formed a rich variety of substrate-mediated structures. For a ~ 4 -ML Sb coverage, the an-

nealed overlayers contained orientationally ordered grains with periodic domain walls and superstructures. The superstructures were modeled as a Moiré effect in which the pseudocubic (110) surface is rotated from the substrate high-symmetry direction. Interestingly, the Sb overlayer grew in multilayers with a height of 6.4 ± 0.5 Å, corresponding to the stacking of three layers perpendicular to the pseudocubic (110) surface with the $\langle 111 \rangle$ direction inclined from the surface normal. For an Sb coverage of 8 ML, the annealed overlayers exhibited structures that were differently oriented than those mediated at low coverage by the substrate with $\langle 111 \rangle$ normal to the surface, thus introducing a grain boundary. Antimony was found to undergo a semiconducting-semimetallic transition at a thickness of ~ 15 Å.

For Bi overlayers on GaAs(110), the first Bi layer grows epitaxially with misfit dislocations. Small triple-layer thick 2D islands grow on the epitaxial monolayer, but these islands are replaced by large crystallites preferentially oriented with respect to the substrate and derived from double-layer structure. Both the 2D islands and the crystallites exhibit one of two differently oriented superstructures. The superstructures were also modeled as a Moiré effect. For thicker films, the Bi crystallites were elongated along the substrate $[1\bar{1}0]$ direction.

It is instructive to compare the results for Sb and Bi for nominal coverages < 6 ML. For an annealing temperature of 525 K and a coverage of 4 ML, Sb formed grains with superstructures and periodically spaced striped domain walls. In this thickness regime, however, Bi formed crystallites containing large grains without striped domain walls, even at 300 K. The larger grain size and the formation of crystallites for Bi at 300 K can be explained by the lower melting temperature of Bi. The formation of domain walls in the Sb overlayer probably reflects the accommodation of strain. In contrast, the lattice constant of Bi is $\sim 5\%$ larger than Sb. The GaAs(110) substrate may expand the Sb lattice by $\sim 5\%$ and strain relief is achieved by the formation of periodic dislocations (striped domain walls). In addition, the Sb (Bi) lattice is rotated by $+7$ ($+10^\circ$) or -7 (-10°) from the substrate symmetry directions. For Sb and Bi on GaAs(110), the angle of rotation then increases for decreasing misfit. This trend is opposite to that predicted by Novaco and McTague²⁶ for orientational epitaxy where the overlayer rotates away from substrate high-symmetry directions, as for rare-gas monolayers adsorbed on graphite where the overlayer rotation decreased as the misfit decreased. Moreover, these semimetals adsorb in multilayers rather than monolayers as for the rare gases. Indeed, they may constitute a new class of materials exhibiting orientational epitaxy.

ACKNOWLEDGMENTS

This work was supported by the National Science Foundation under Grant No. DMR-8610837. Helpful discussions with Y.-J. Hu are gratefully appreciated. D. Owens generously offered technical assistance.

- ¹See, for example, *Proceedings on the Fifth International Conference on Scanning Tunneling Microscopy/Spectroscopy* [J. Vac. Sci. Technol. B **9**, 403 (1991)]. See also J. H. Weaver, in *Electronic Materials: A New Era of Materials Science*, edited by J. R. Chelikowsky and A. Franciosi (Springer-Verlag, Berlin, 1991), Chap. 8, pp. 135–214.
- ²R. M. Feenstra and P. Mårtensson, Phys. Rev. Lett. **61**, 447 (1988); P. Mårtensson and R. M. Feenstra, Phys. Rev. B **39**, 7744 (1989).
- ³C. K. Shih, R. M. Feenstra, and P. Mårtensson, J. Vac. Sci. Technol. A **8**, 3379 (1990).
- ⁴A. B. McLean, R. M. Feenstra, A. Taleb-Ibrahimi, and R. Ludeke, Phys. Rev. B **39**, 12 925 (1989); J. Vac. Sci. Technol. B **7**, 936 (1989).
- ⁵Y. Hu, M. B. Jost, T. J. Wagener, and J. H. Weaver, Phys. Rev. B **42**, 7050 (1990); J. Vac. Sci. Technol. B **9**, 255 (1991).
- ⁶Y. Hu, T. J. Wagener, M. B. Jost, and J. H. Weaver, Phys. Rev. B **40**, 1146 (1989).
- ⁷G. D. Waddill, C. M. Aldao, C. Capasso, P. J. Benning, Y. Hu, T. J. Wagener, M. B. Jost, and J. H. Weaver, Phys. Rev. B **41**, 5960 (1990).
- ⁸J. J. Joyce, J. Anderson, M. M. Nelson, and G. J. Lapeyre, Phys. Rev. B **40**, 10 412 (1989); J. Vac. Sci. Technol. A **7**, 850 (1989); **8**, 3542 (1990).
- ⁹J. C. Patrin, Y. Z. Li, M. Chander, and J. H. Weaver, Phys. Rev. B **45**, 3918 (1992).
- ¹⁰F. Jona, Surf. Sci. **8**, 57 (1967).
- ¹¹F. Schaffler, R. Ludeke, A. Taleb-Ibrahimi, G. Hughes, and D. Rieger, Phys. Rev. B **36**, 1328 (1987); J. Vac. Sci. Technol. B **5**, 1048 (1987).
- ¹²R. Stümppler and H. Lüthe, Surf. Sci. **182**, 545 (1987).
- ¹³For a review of domain walls, see M. den Nijs, in *Phase Transitions*, edited by C. Domb and J. L. Lebowitz (Academic, New York, 1988), Vol. 12, Chap. 2; P. Bak, Rep. Prog. Phys. **45**, 587 (1982).
- ¹⁴D. E. Savage and M. G. Lagally, Appl. Phys. Lett. **50**, 1719 (1987).
- ¹⁵V. B. Sandomirskii, Zh. Eksp. Teor. Fiz. **25**, 158 (1967) [Sov. Phys.—JETP **52**, 101 (1967)].
- ¹⁶S. Takaoka and K. Murasi, J. Phys. Soc. Jpn. **54**, 2250 (1985).
- ¹⁷M. S. Dresselhaus, in *The Physics of Semimetals and Narrow-Gap Semiconductors*, edited by D. L. Carter and R. T. Bate (Pergamon, New York, 1971), p. 18.
- ¹⁸C. B. Duke, D. L. Lessor, T. Guo, and W. K. Ford, J. Vac. Sci. Technol. A **8**, 3412 (1990).
- ¹⁹M. Prietsch, A. Samsavar, and R. Ludeke [Phys. Rev. B **43**, 11 850 (1991)] have reported islands of similar heights for Bi grown on GaP(110).
- ²⁰U. Resch, N. Esser, and W. Richter, Surf. Sci. **251/252**, 621 (1991); N. Esser, M. Hünernman, U. Resch, D. Spaltmann, J. Geurts, D. R. T. Zahn, W. Richter, and R. H. Williams, Appl. Surf. Sci. **41/42**, 169 (1989).
- ²¹A. B. McLean and F. J. Himpsel, Phys. Rev. B **40**, 8425 (1989).
- ²²The surface unit cell (two atoms) of the pseudocubic (110) plane [$(10\bar{1})$ in rhombohedral coordinates] is 6.572 Å in the $\langle 100 \rangle$ direction and 4.746 in the $\langle 110 \rangle$ direction. In the $\langle 001 \rangle$ direction the average spacing is 6.572/2 Å or 3.29 Å.
- ²³J. Donohue, in *Structures of the Elements* (Wiley, New York, 1982), p. 308.
- ²⁴R. J. Needs, R. M. Martin, and O. H. Nielsen, Phys. Rev. B **33**, 3778 (1986); **35**, 9851 (1987).
- ²⁵L. F. Vereshchagin and S. S. Kabalkina, Zh. Eksp. Teor. Fiz. **47**, 414 (1964) [Sov. Phys.—JETP **20**, 274 (1964)].
- ²⁶A. D. Novaco and J. P. McTague, Phys. Rev. Lett. **38**, 1286 (1977); Phys. Rev. B **19**, 5299 (1979).

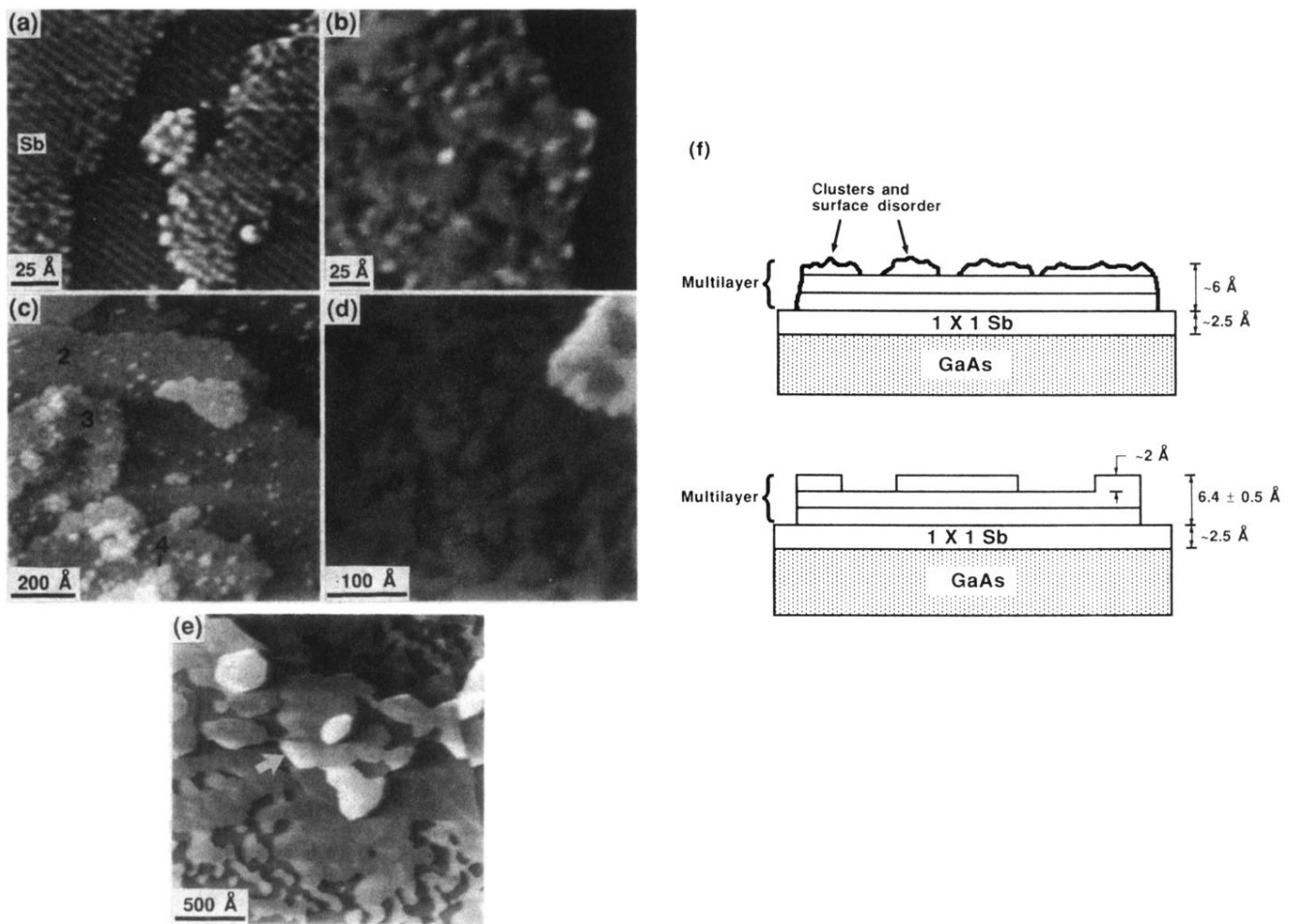


FIG. 1. (a) A curvature-enhanced atomic resolution image obtained after the equivalent of 0.5 ML of Sb was deposited at 575 K on GaAs(110). The islands at the left and right exhibit the 1×1 epitaxial Sb structure. Growth at 300 K produces clusters on the 1×1 structure and at the edges of the 1×1 islands, but the cluster number density is significantly reduced for growth at 575 K. (b) 200×200 -Å² image showing the growth of an Sb multilayer on the 1×1 Sb epilayer (the latter is the underexposed region at the right of the image). The multilayer surface shows disorder due to depressions (darker regions) and Sb clusters (bright spots). This layer is ~ 6 Å thick, corresponding to three layers of Sb. (c) STM image after the equivalent of 4 ML Sb was deposited on GaAs(110) at 300 K. The upper right corner shows the 1×1 epilayer with bright spots that correspond to islands of the first multilayer. The numbers draw attention to four successive multilayers. Each is ~ 6 Å thick, corresponding to a triple layer of Sb. Small clusters are also apparent on each multilayer surface. (d) A 400×400 -Å² image obtained after annealing the surface of Fig. 1(c) to 375 K. Annealing eliminates the small Sb clusters and enhances surface ordering. The darker regions are recessed by a single Sb layer from the surrounding regions. The brighter area at upper right shows a second trilayer where the darker portions are one layer thinner. (e) STM image after annealing 4 ML of Sb at 500 K. The dark areas in the lower half reflect ordered regions one Sb layer thinner than the brighter areas surrounding them. The upper portion shows a large island that is 6.4 Å thick and derived from a triple layer of Sb, as indicated by the arrow. Within it, the darker areas are two layers thick. Comparison to (d) shows that annealing enhances layer ordering by forming a complete atomic layer near the trilayer island. (f) A schematic cross section depicting Sb multilayer growth on a 1×1 epilayer on GaAs(110). The upper panel reveals the disorder apparent in the images of (b) and (c). Annealing produces the better ordered structure of the lower panel with double and triple layers of Sb on the 1×1 layer.

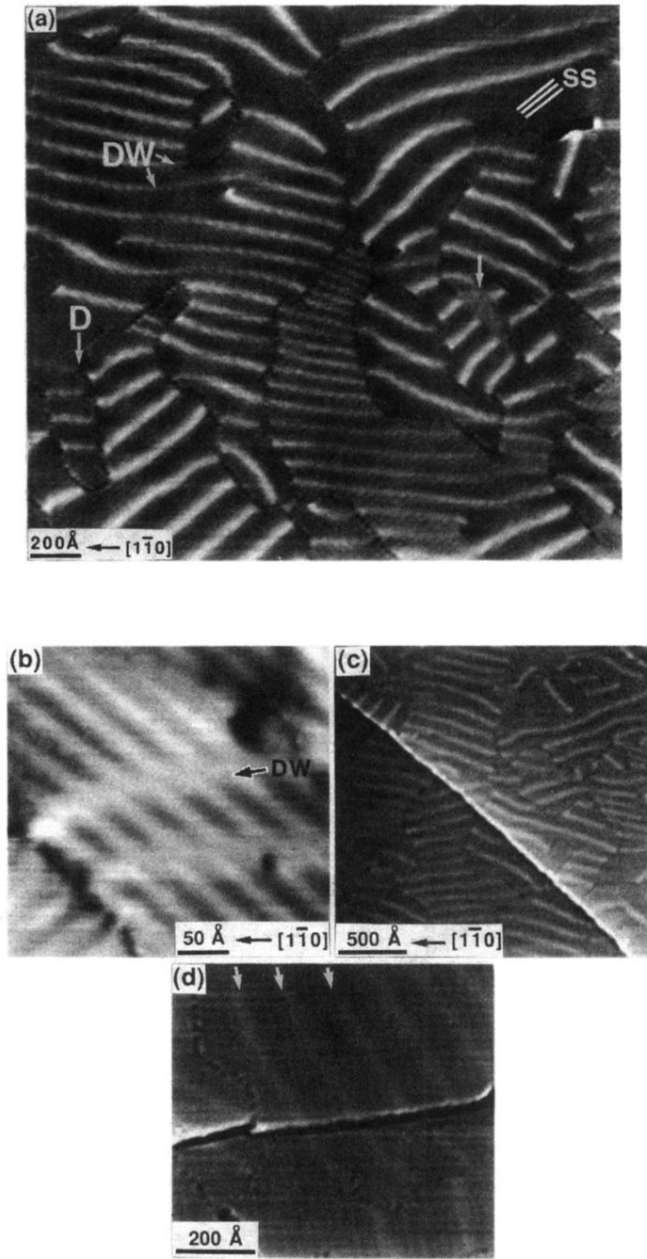


FIG. 2. (a) STM image obtained after annealing 4 ML of Sb to 525 K for 2 h. Differently oriented superstructures (SS) aligned $+40^\circ$ or -40° relative to the substrate $[1\bar{1}0]$ direction are apparent in the grains as straight lines in gray scale. As discussed, the superstructure reflects a Moire effect. Defects (D) of ~ 20 -Å size define the grain boundaries. Periodically spaced striped domain walls (DW) are formed within each grain due to strain in the Sb overlayer. The dark region at upper right is a monolayer depression. The arrow draws attention to a region with no apparent order. (b) STM image of a portion of (a) showing a grain defined by defects with domain walls and a superstructure that is oriented 40° relative to $[1\bar{1}0]$. There is a phase shift of 180° as the superstructure passes through the domain wall. (c) A curvature-enhanced STM image showing that the grain boundaries and the domain walls are continuous over a monatomic substrate step which runs diagonally through the image. (d) A curvature-enhanced STM image showing that the domain walls (marked by arrows) continue through a 6.4-Å-high multilayer step in the Sb overlayer.

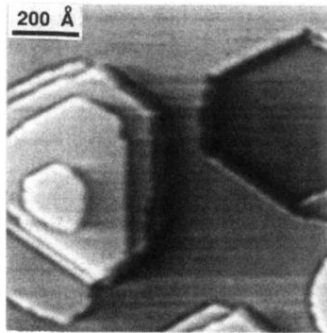


FIG. 4. STM image obtained after 10-ML Sb deposition on GaAs(110) followed by annealing to 475 K. The left portion shows an island consisting of four Sb bilayers. Each bilayer is ~ 4 Å high. The Sb rhombohedral $\langle 111 \rangle$ direction is normal to the surface. The hexagonal pit at the right is two bilayers or ~ 8 Å deep.

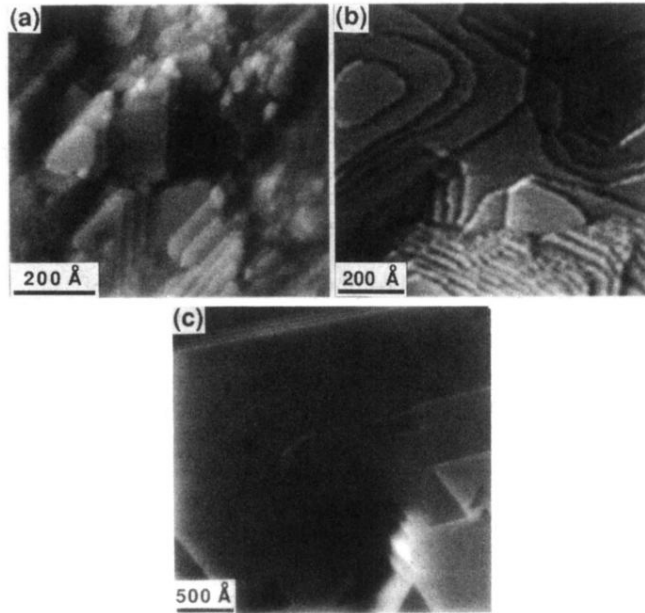


FIG. 5. (A) $800 \times 800\text{-}\text{\AA}^2$ STM image of 20 ML of Sb deposited at 300 K. The triangular structures expose $\{111\}$ surfaces that are randomly oriented. (b) $1000 \times 1000\text{-}\text{\AA}^2$ curvature-enhanced image obtained after annealing (a) to 500 K. The top portion shows Sb crystallites with basal planes parallel to the substrate. Each layer is $\sim 4\text{ \AA}$ thick, and ten layers can be seen in this image. The bottom portion shows a stack of layers in which the $\langle 111 \rangle$ direction is not normal to the surface. (c) STM image showing 20 ML of Sb after annealing to 600 K. The $\langle 111 \rangle$ direction of the overlayer is normal to the surface. In general, the surface is very flat, but triangular-shaped structures can be observed that are related to pairs of clockwise and counterclockwise screw dislocations. In addition, triangular-shaped pits can also be observed (not shown here). Each layer is $3.9 \pm 0.4\text{ \AA}$ thick, corresponding to two Sb layers.

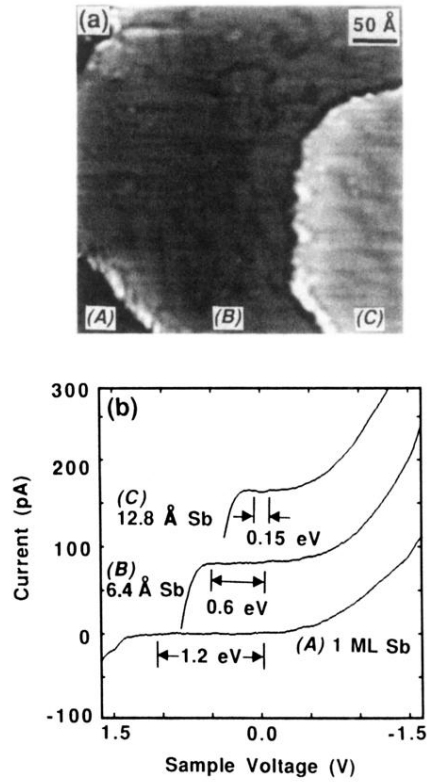


FIG. 6. (a) $400 \times 400 \text{-}\text{\AA}^2$ STM image for ~ 3 ML of Sb annealed to 425 K. The image shows two successive ~ 6 -high- \AA -trilayers (*B* and *C*) on the 1×1 layer (*A*). (b) Representative I - V curves labeled *A*, *B*, and *C* correspond to measurements taken at the 1×1 Sb layer (*A*), the 6.4- \AA trilayer (*B*), and the 12.8- \AA trilayer (*C*) showing a reduction in the band gap as the Sb layer thickens. Sb undergoes a semiconductor-semimetal transition at $\sim 15 \text{\AA}$.

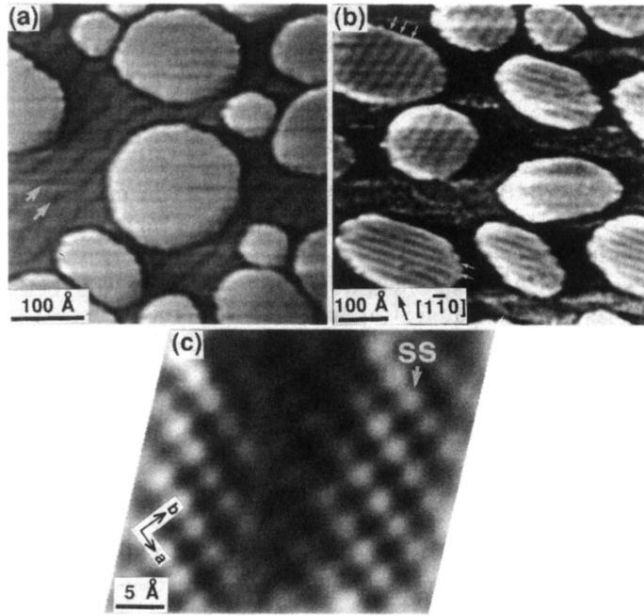


FIG. 7. (a) $450 \times 450\text{-}\text{\AA}^2$ curvature-enhanced image showing 2-ML Bi deposition at 300 K (sample bias of 1.47 V). The lower level reflects the 1×1 epitaxial layer with periodic misfit dislocations (arrows) spaced about 25 \AA in the $[1\bar{1}0]$ direction. The islands on the epilayer are $\sim 7\text{ \AA}$ high and nearly isotropic. (b) $750 \times 750\text{-}\text{\AA}^2$ image obtained with a sample bias of -0.1 V that reveals the two differently oriented periodic superstructures on the island surface. The superstructure is oriented $+55\%$ or -55% from the substrate $[1\bar{1}0]$ direction. This image has not been drift-corrected. (c) Drift-corrected atomic resolution image of $\sim 7\text{-}\text{\AA}$ -high Bi island. The lattice spacing is 3.4 and 4.5 \AA in the a and b directions. Notice that the rows shift by one half the lattice spacing as they pass through the superstructure (SS).

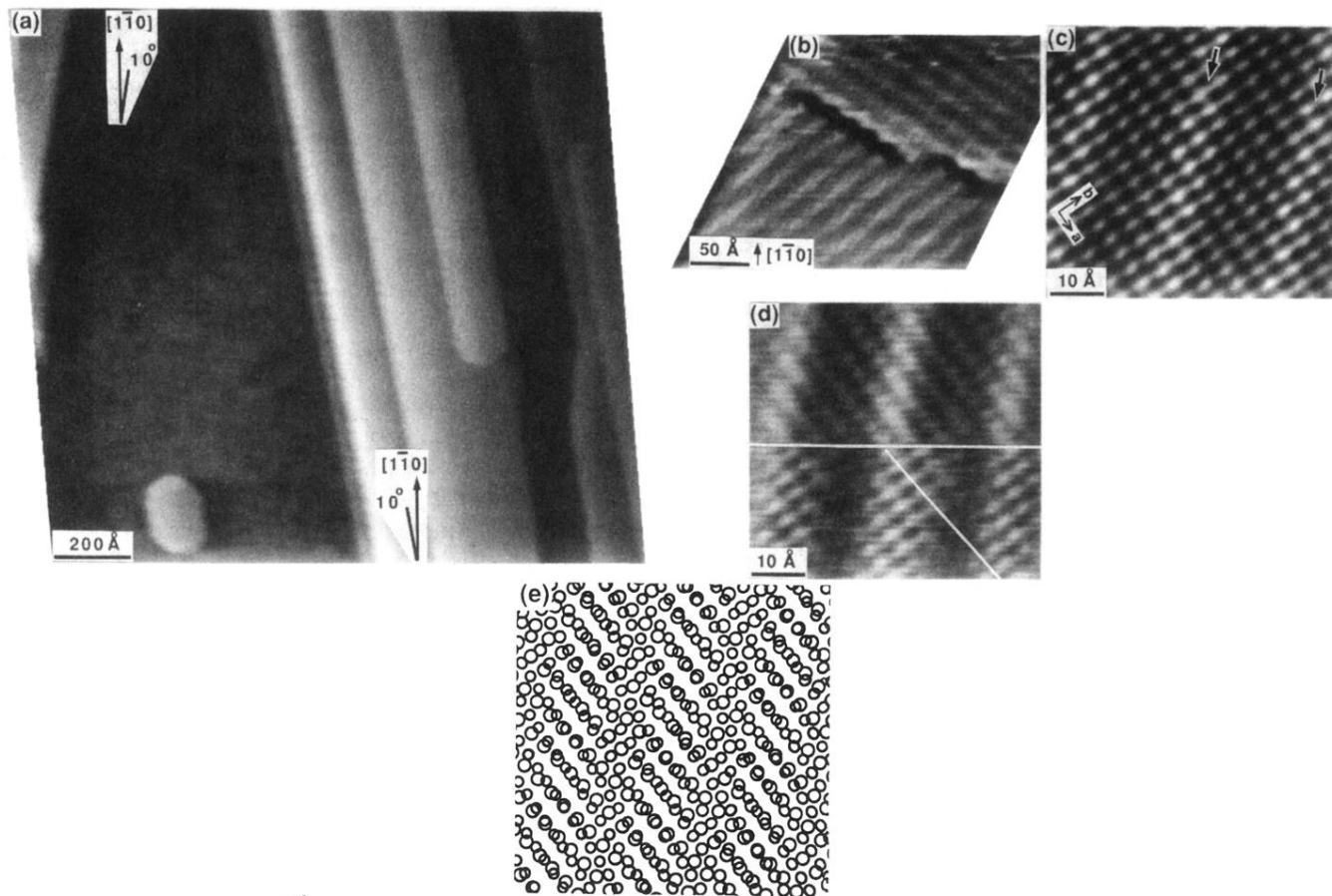


FIG. 8. (a) $1400 \times 1400\text{-}\text{\AA}^2$ image for 6-ML Bi deposition at 300 K. The image shows elongated Bi crystallites aligned $+10^\circ$ or -10° from the substrate $[1\bar{1}0]$ direction. Within the crystallites, there are $21\text{-}\text{\AA}$ periodic superstructures oriented $+55^\circ$ or -55° from the $[1\bar{1}0]$ direction as in Fig. 7(b). Each step within the crystallite corresponds to a Bi bilayer ($\sim 4\text{ \AA}$). The isolated Bi island at the lower left corner of the figure is $\sim 7\text{ \AA}$ high. It also contains a periodic superstructure. (b) Higher-resolution image showing the two superstructure orientations separated by a line of defects. The superstructures are oriented either $+55^\circ$ or -55° from the $[1\bar{1}0]$ substrate direction. (c) Atomic resolution image of a Bi crystallite after 6 ML of Bi was deposited at 300 K. The atomic spacing is 3.25 \AA along the a direction and 4.66 \AA along the b direction. The arrows draw attention to the periodic superstructure. (d) Atomic resolution image showing the bias dependence for rows as they pass through the superstructure. The rows in the upper portion of the image appear to run straight through the superstructure (bias 90 mV), whereas those at the bottom appear to shift by one half the lattice spacing (bias 30 mV), as indicated by the white line. (e) Moiré pattern generated by rotating the $\langle 001 \rangle$ direction of the pseudocubic (110) Bi pseudocubic lattice by -10° relative to the $[1\bar{1}0]$ substrate direction. The superstructure appears as periodically spaced lines running -55° from the $[1\bar{1}0]$ substrate direction.

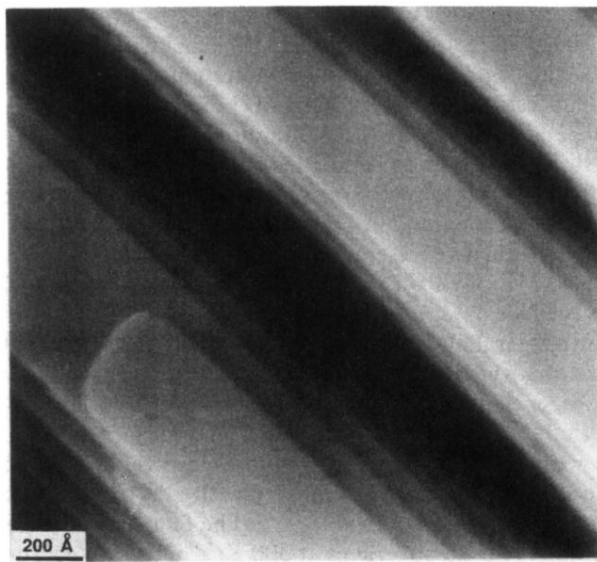


FIG. 9. STM image obtained after 50 ML of Bi deposition at 300 K. The Bi crystallites have atomically flat surfaces and elongate preferentially along the substrate $[1\bar{1}0]$ direction. Each layer is ~ 4 Å thick, corresponding to stacking of two layers in the $\langle 111 \rangle$ rhombohedral direction.